Journal of the Korea Concrete Institute
Vol.17 No.5, pp.843~852, October, 2005

Uniaxial Compression Behavior of High-Strength Concrete Confined by Low-Volumetric Ratio Lateral Ties

Ki-Nam Hong[1)*] and Sang-Hoon Han[1)]

[1)] Dept. of Civil Engineering, Chungbuk National University, 361-240, Korea

(Received February 24, 2005, Accepted July 14, 2005)

Abstract

Presently, test results and stress-strain models for poorly confined high-strength columns, more specifically for columns with a tie volumetric ratio smaller than 2.0%, are scarce. This paper presents test results loaded in axial direction for square reinforced concrete columns confined by various volumetric ratio lateral ties including low-volumetric ratio. Test variables include concrete compressive strength, tie yield strength, tie arrangement type, and tie volumetric ratio. Local strains measured using strain gages bonded to an acryl rod. For square RC columns confined by lateral ties, the confinement effect was efficiently improved by changing tie arrangement type from Type-A to Type-B. A method to compute the stress in lateral ties at the concrete peak strength and a new stress-strain model for the confined concrete are proposed. Over a wide range of confinement parameters, the model shows good agreement with stress-strain relationships established experimentally.

Keywords: high-strength concrete, column, low-volumetric ratio, localized region length, stress-strain curve

1. Introduction

To date, the lateral confining pressure p has been formulated by multiplying the yield strength by area or volumetric ratio of ties. Namely, when a higher-grade tie is also used, the confining pressure is calculated using the tie yield strength f_{sy} predicting the higher confining pressure. However, in previous studies,[2)] test results showed that in HSC the higher-grade tie at the peak strength does not yield. In addition, depending on the confinement efficiency and grade of steel, the lateral ties of columns using high-strength materials may or may not yield; we cannot assume that lateral ties in poorly confined columns will yield. Therefore, in HSC, the tie yield strength cannot be used when calculating the confinement pressure, since the confinement calculation using f_{sy} will overestimate the lateral confining pressure. For design convenience, the Japan's new project[3)] recommends using tie yield strengths of 700 and 1100 MPa as the upper limit, respectively, for rectangular and circular cross-section. Namely, when a lateral tie exceeding the upper limit is used, it is possible to prevent from overestimating the confinement effect by substituting the limit value for the tie yield strength. Currently, however, the background is not clearly found out. Notably, test results and stress-strain models for poorly confined high-strength columns, more specifically, for columns with a tie volumetric ratio smaller than 2.0% (i.e., the case of RC bridge pier's design),[4)] are extremely scarce. In order to calculate the accurate confining pressure, it is necessary to determine the real stress in lateral ties at the concrete peak strength $f_{s,cal}$. To solve the problems delineated in the previous sections, a total of 34 square RC columns were tested in this study. The following variables were considered to evaluate the effect of confinement on the stress-strain relationship of the confined concrete: concrete compressive strength, tie yield strength, tie arrangement type, and tie volumetric ratio. Relative to previous research,[5)-7)] specimens in this study have smaller lateral tie volumetric ratios. Based on the experimental results, a method to compute the stress in lateral ties at the concrete peak strength and a stress-strain model are proposed, which are applicable to the wide range of test variables of this study. This study is a follow up to the previous research performed by Hong et al..[2)] And, for more generalization,

* *Corresponding author*
Email address: hong@chungbuk.ac.kr

Table 1 Specimen details and test results

Notation of specimens	f_c' [a] (MPa)	Lateral tie					Test reuslts			
		d (mm)	s (mm)	ρ_s (%)	f_{sy} [b] (MPa)	Tie arrangement[d]	f_{cc} (MPa)	ε_{cc} (%)	$f_{s,exp}$ [e] (MPa)	ε_{50} (%)
SF1P0Y0-4	39.2	—	—	—	—	—	33.9	0.27	—	0.41
SF1P0Y0-5		—	—	—	—	—	35.7	0.29	—	0.39
SF1P0Y0-6		—	—	—	—	—	33.1	0.28	—	0.42
TF1P1Y1		6.0	40	2.16	379	Type-B	47.4	0.59	379	6.50
TF1P1Y4		6.4	40	2.05	1420	Type-B	52.8	1.77	583	8.31
TF1P2Y1		6.0	85	1.02	379	Type-B	39.9	0.38	478	2.02
TF1P2Y4		6.4	85	0.96	1420	Type-B	42.4	0.39	404	2.15
TF1P3Y1		6.0	150	0.58	379	Type-B	39.4	0.34	586	0.61
TF1P3Y4		6.4	150	0.55	1420	Type-B	39.1	0.36	347	1.33
SF1P2Y4		6.4	40	1.20	1420	Type-A	39.5	0.37	299	2.01
SF1P3Y4		6.4	60	0.80	1420	Type-A	39.1	0.41	336	1.23
DF1P2Y4[c]		6.4	120	0.91	1420	Type-A	39.8	0.34	206	1.15
SF2P0Y0-4	80.0	—	—	—	—	—	62.1	0.29	—	0.36
SF2P0Y0-5		—	—	—	—	—	60.9	0.32	—	0.38
SF2P0Y0-6		—	—	—	—	—	65.4	0.35	—	0.40
TF2P1Y1		6.0	40	2.16	379	Type-B	96.9	0.44	318	0.91
TF2P1Y4		6.4	40	2.05	1420	Type-B	101.0	0.42	358	2.63
TF2P2Y1		6.0	85	1.02	379	Type-B	81.2	0.37	379	0.95
TF2P2Y4		6.4	85	0.96	1420	Type-B	85.1	0.42	494	1.26
TF2P3Y1		6.0	150	0.58	379	Type-B	75.4	0.29	379	0.38
TF2P3Y4		6.4	150	0.55	1420	Type-B	75.1	0.35	594	0.87
SF2P2Y4		6.4	40	1.20	1420	Type-A	72.8	0.33	575	0.75
SF2P3Y4		6.4	60	0.80	142	Type-A	79.2	0.37	405	0.75
DF2P2Y4[c]		6.4	120	0.91	1420	Type-A	79.3	0.40	526	0.70
SF3P0Y0-4	116.0	—	—	—	—	—	83.4	0.33	—	0.39
SF3P0Y0-5		—	—	—	—	—	82.6	0.30	—	0.39
SF3P0Y0-6		—	—	—	—	—	92.0	0.33	—	0.37
TF3P1Y1		6.0	40	2.16	379	Type-B	121.4	0.38	379	0.75
TF3P1Y4		6.4	40	2.05	1420	Type-B	123.1	0.39	606	2.00
TF3P2Y1		6.0	85	1.02	379	Type-B	102.4	0.38	340	0.46
TF3P2Y4		6.4	85	0.96	1420	Type-B	105.6	0.38	497	0.88
TF3P3Y1		6.0	150	0.58	379	Type-B	105.1	0.34	379	0.37
TF3P3Y4		6.4	150	0.55	1420	Type-B	111.3	0.35	637	0.45
SF3P2Y4		6.4	40	0.91	1420	Type-A	97.5	0.33	375	0.53

[a] *The average compressive strength obtained from three cylinders (ϕ 100×200 mm),* [b] *The average yield strength obtaine* from three specimens

[c] The column having double layers' rectangular ties, [e] The real stress in lateral ties at the concrete peak strength

[d]

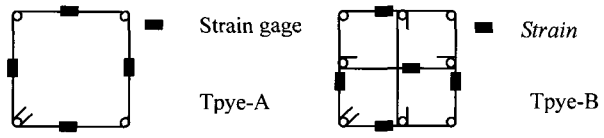

test results from Hong et al.[2] are also considered in this study.

2. Experimental program

2.1 Specimen properties and materials

All tested specimens were 250 mm×250 mm square sections, 750 mm in height. The test parameters included expected concrete compressive strengths f_c' (40, 80, and 120 MPa), tie volumetric ratios ρ_s (0.55%, 0.58%, 0.80% 0.91%, 0.96%, 1.02%, 1.20%, 2.05%, and 2.16%), yield strength of lateral ties f_{sy} (379 and 1420 MPa), and rectangular ties' arrangement types (Type-A and Type-B). Specimen details are listed in Table 1. Stress-strain relationships, established by performing coupon test for each reinforcement, are illustrated in Fig. 1. SD295 was used as longitudinal bars in all specimens. The diameter of the lateral ties was approximately 6 mm (for more details, see Table 1). In all confined specimens, the spacing of lateral ties was reduced to 15 mm in the two end regions to provide sufficient confinement and to eliminate failure at the

Table 2 Concrete mixture proportions

f_c' (MPa)	G_{max} (mm)	w/c (%)	s/a (%)	Unit weight (kg/m^3)							
								G		Agent	
				W	C	Ad[a]	S	5-10 (mm)	10-15 (mm)	water-reducing agent	air-entraining admixture
39.2	15	40	47	164	410	0	856	382	574	1.64	0.16
80.0	15	27	36	166	572	55.2[b]	599	429	529	8.58[c]	
116.0	15	22	42	149	703	100[d]	697	388	582	7.70[c]	

[a] Admixture , [b] High performance admixture, [c] High performance water-reducing agent, [d] Silica fume

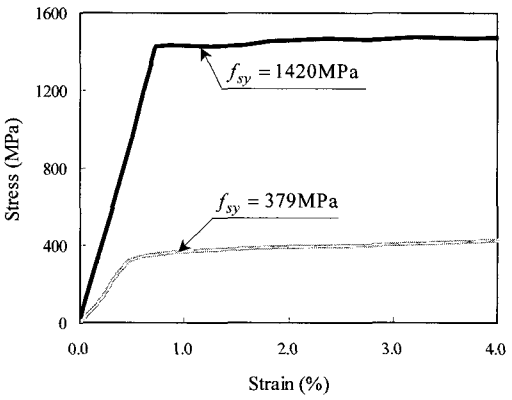

Fig. 1 Stress-strain relationship of lateral reinforcement

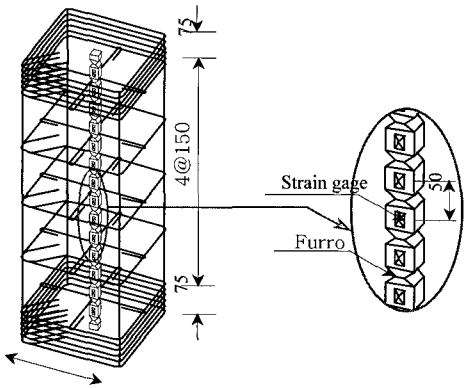

Fig. 2 Detail of reinforcement, acryl rod, and strain gage position for specimen TF1P3Y4 (unit: mm)

two end sections of the specimen. Consequently, the specimens were forced to fail in the middle section. All lateral ties were anchored by 135-degree hooks around one of the longitudinal bars, extending 60 mm into the concrete core.

To evaluate the post-peak behavior of confined HSC columns in real structures, it is necessary to study the crack localization of columns, which is compression loaded in axial direction. The measurement technique of strains using a deformed acryl rod embedded within concrete columns, which is introduced by Nakamura and Higai,[8] was found to be effective and was also adopted in this study. The acryl rod with a square cross-section of 10 mm×10 mm was first deformed by introducing triangle-shaped furrows at four side faces in order to ensure good bonding between the acryl rod and concrete, as shown Fig. 2. Strain gages were attached to the rod, which was then installed vertically in a position coincident with the specimen's centerline before casting of the concrete. Detail of reinforcement, acryl rod, and strain gage position for specimen TF1P3Y4 is shown in Fig. 2.

The specimens were cast from three batches. Mixture proportions for concrete used in this study are given in Table 2. Type I Ordinary Portland cement (OPC) is used in all mixtures. Crushed gravel is used as the coarse aggregate and the maximum aggregate size G_{max} is 15 mm. The concrete compressive strength was determined based on the average of three identical ϕ 100×200 mm cylinders from the same batch (see Table 1). Also, three plain concrete columns per batch (e.g., SF1P0Y0-4) were prepared as unconfined concrete specimens to obtain the in-place compressive strength of the unconfined concrete f_{c0}'. In the following sections, these batches are referred to by their group number F, such that F1 denotes f_c' = 39.2 MPa, F2 denotes f_c' = 80.0 MPa, and F3 denotes f_c' = 116.0 MPa.

2.2 Testing procedure and instrumentation

A concentric compressive load was applied using a hydraulic universal testing machine (UTM) with a capacity of 10 MN. An overall view of the test specimen set up is shown in Fig. 3. It is generally accepted that HSC should be tested using a very rigid machine.[9] The steel reaction columns of the machine used in this study are stiff enough to meet such requirements and permit the machine to load the specimen at a rate as low as 0.01 mm/min. This was achieved using displacement-controlled testing and displacement increment was 0.2~0.3 mm/min to approximately 80% point of the maximum load. However, after the point, the displacement increments were gradually reduced (i.e., 0.01~0.3 mm/min) to measure a softening behavior.

The axial deformation of the specimens was obtained us-

ing four linear variable differential transducers (LVDTs) located at each corner of the specimen. LVDTs with a gage length of 750 mm were attached to the platen and crosshead. The overall concrete axial strain was calculated as the average of the LVDT measurements divided by the gage length. Steel strains were measured until the specimen failed using electrical resistance strain gages bonded to the lateral ties. Strains in lateral ties for ties' arrangement type-A and type-B were measured using 4 and 6 strain gages, respectively, as shown in Table 1. Longitudinal local strains in concrete were measured using 15 strain gages bonded to the acryl rod at intervals of 50 mm as shown in Fig. 2. In addition, loads were measured continuously using a load cell. Crack pattern, buckling of axial reinforcement, and other observational data were also recorded during all tests.

3. Analysis of test results

3.1 Failure mode

For group F1 specimens, the minimum strength enhancement ratio was 1.14 [(TF1P3Y4, ρ_s =0.55%) and (SF1P3Y3, 0.80%)], while the maximum ratio was 1.54 (TF1P1Y4, ρ_s =2.05%). Vertical cracks occurred at the corners of specimens from zero to peak load. More specifically, after the strain corresponding to the yield strength of longitudinal bar, a lot of cracks happened at the cover concrete until the peak load. At the peak load, due to the sudden spalling of the concrete cover, F1 specimens lost approximately 7~13% values of the maximum strength. Beyond the peak load point, the strength of specimen TF1P1Y4 having the closest lateral tie spacing increased until second peak point and the core concrete was almost sound (see Fig. 4(a)). On the other hand, the strength of specimen TF1P3Y4 having the widest tie spacing decreased very fast due to crushing of the concrete cover. The damage was concentrated between tie bars and the core concrete was significantly damaged due to the apparent buckling of longitudinal bars (Fig. 4(b)). The strength enhancement ratio of group F2 specimens was a minimum of 1.17 (SF2P2Y4, ρ_s =1.2%) and a maximum of 1.62 (TF2P1Y4, ρ_s =2.05%). Although specimens of group F2 failed in the same manner as specimens of group F1, specimens of group F2 showed more rapid reduction in load-carrying capacity due to spalling of the concrete cover. More specifically, after the lose of the sudden load-carrying, the strength of specimen TF2P1Y4 decreased due to spalling of the concrete cover and kept the almost constant strength during the additional increment of axial displacement (i.e., 4 mm). After that, its strength gradually decreased. When we compare specimens having an equal confinement and close spacing from groups F1 and F2, it is noted that the damage of the core concrete is similar and the difference is insignificant (i.e., Figs. 4(a) and (c)). On the other hand, when the tie spacing is wide, the core concrete of group F2 specimens is damaged more significantly than that of group F1 specimens. Also, the failure of group F2 specimens was relatively sudden and explosive.

The strength enhancement ratio of group SF3 specimens was a minimum of 1.15 (SF3P2Y4, ρ_s =0.91%) and a maximum of 1.45 (TF3P1Y4, ρ_s =2.05%). All specimens of group F3 exhibited more brittle failure than that of

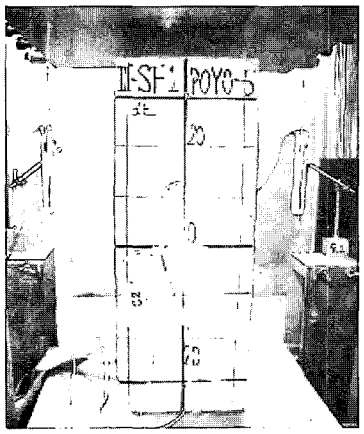

Fig. 3 Overall view of test set-up

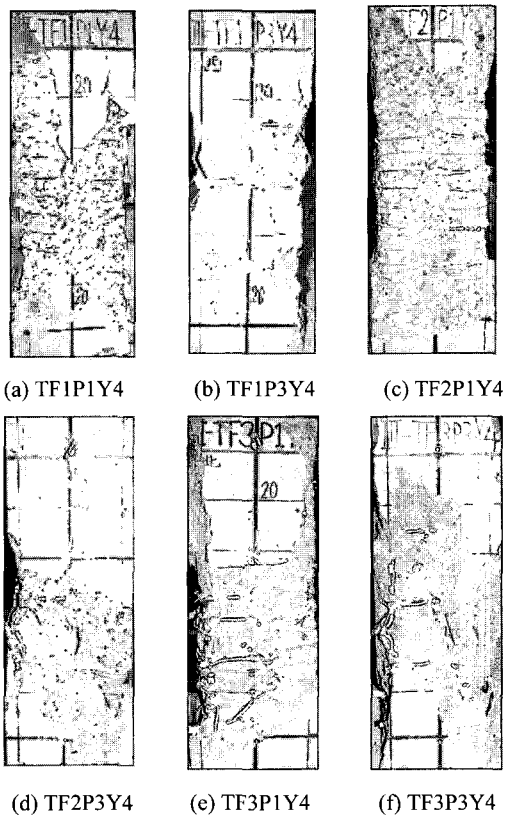

(a) TF1P1Y4 (b) TF1P3Y4 (c) TF2P1Y4

(d) TF2P3Y4 (e) TF3P1Y4 (f) TF3P3Y4

Fig. 4 Specimens after testing

groups F1 and F2. Except for specimens TF3P1Y4 and TF3P2Y4, after the peak strength, all specimens lost explosively the load resistance after the spalling of concrete. Meanwhile, the specimen TF3P1Y4 lost the load resistance of approximately 10% and, as a result, failed slowly. When we compare specimens having the same spacing from groups F2 and F3, it is found that the damage of specimen TF3P1Y4 was concentrated in the narrower region. For all specimens, a well-defined shear failure plane was formed after one or two of lateral ties ruptured.

4. Discussion of test results

4.1 Local strain distribution

The local strains of the confined column under uniaxial compression were measured by using strain gages bonded to the acryl rod. Fig. 5 shows the local stress-strain curves and the appearance after testing of specimens TF1P2Y4, TF2P1Y4, and TF3P1Y4. Also, the numbers marked in Fig. 5 denote the numbers corresponding to 15 strain gages. It can be seen from Fig. 5 that, for the descending branch after the peak strength, some parts of the specimen show the continuous increase of strains while others show the decrease of strains and the ductility decreases as the compressive strength increases. The damaged zone after testing of specimens almost coincided with increasing parts of strains. Accordingly, it can be concluded that the technique measuring local strains by embedding a deformed acryl rod adopted in this study is effective to capture the localized compressive failure behavior of the confined RC column, although the measuring accuracy after fracture of one or two ties is not sufficient due to the occurrence of the shear failure plane.

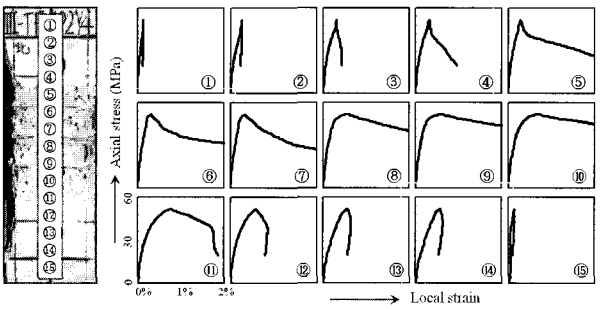

(a) TF1P2Y4

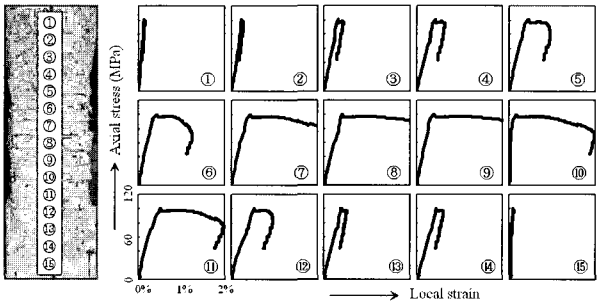

(b) TF2P1Y4

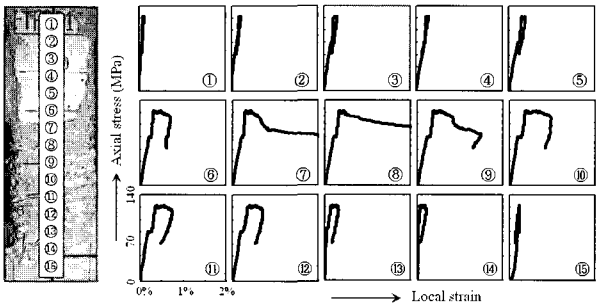

(c) TF3P1Y4

Fig. 5 Distribution of axial stress with local strain

In this paper, the strain increasing and decreasing zones were defined as the failure zone and unloading zone, respectively. The failure zone of specimens decreases as the concrete strength increases as shown in Fig. 5. This means that, when the HSC is used, the failure was localized into some parts inside the specimen compared to NSC and hence the ductility of specimen decreases. All test results show that the failure zone increases when the volumetric ratio of lateral ties increase and when the higher-grade tie is used. Consequently, it can be concluded that the localization phenomenon of the confined RC column is directly related to the effective confining pressure.

4.2 Effect of the yield strength of lateral ties

Fig. 6 shows the stress-strain curves of specimens with volumetric ratio (approximately 0.6%, 1.0%, and 2.1%) for three concrete strengths. For each pair, specimens have different tie yield strengths and the same tie arrangement of Type-B. For all specimens, no increase in the strength enhancement and strain corresponding to the peak strength are shown when the tie yield strength is increased from 379 MPa to 1420 MPa.

This is because when higher-grade ties are used the stress in the lateral tie at the concrete peak strength is less than 50% of the tie yield strength. From this result, it is noted that an increase of lateral tie grade cannot compensate for the proportional reduction in the volumetric ratio for poorly confined columns like specimens of this study.

Generally, the lateral confining pressure at the peak strength is calculated using the tie yield strength, predicting higher confining pressures when a higher-grade tie is used. However, in the previous study,[1)] test results show that in HSC the higher-grade tie does not yield. Therefore, in HSC, the tie yield strength cannot be used when calculating the

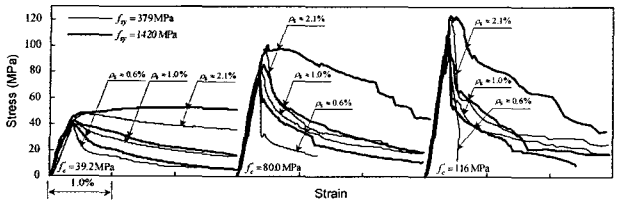

Fig. 6 Effect of tie yield strength f_{sy} on the stress-strain curve

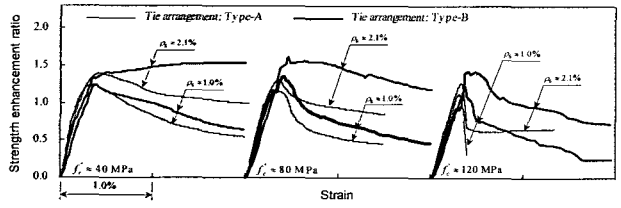

Fig. 7 Effect of tie arrangement on the strength enhancement ratio

confinement pressure, since the confinement calculation using f_{sy} will overestimate the lateral confining pressure. In order to calculate the accurate confining pressure, it is necessary to determine the real stress in lateral ties at the concrete peak strength; this is discussed in the "Stress in lateral ties at the concrete peak strength, $f_{s,cal}$" section.

On the other hand, the behavior after the peak strength is different from that at the peak strength with increasing of tie yield strength. When the tie yield strength is increased from 379 MPa to 1420 MPa, the ductility enhancement of specimens having compressive strength of 39.2 MPa is not significant. For specimens having compressive strengths of 80.0 and 116.0 MPa, however, the ductility of specimens having volumetric ratio of 2.1% is significantly improved and the ductility of specimens having lower volumetric ratios than 2.1% is slightly increased as the tie yield strength increases.

4.3 Effect of the lateral tie arrangement type

Fig. 7 shows the stress-strain curves of specimens with volumetric ratio (approximately 1.0% and 2.1%) for three concrete strengths. For each pair, specimens have tie arrangements of Type-A and Type-B and almost the same compressive strength. Where the tie yield strengths are 1288 and 1420 MPa, respectively, for tie arrangements Type-A and Type-B.

The specimens with tie arrangement of Type-A are selected from reference 2. For specimens made of NSC, when tie arrangement Type-B instead of Type-A is used, no increase in the strength enhancement ratio and the strain at the peak strength is obtained. However, the behavior after the peak strength is significantly developed.

On the other hand, columns made of HSC show higher strength enhancement ratios and ductility enhancement than that of NSC. More specifically, specimens having concrete compressive strength of approximately 120 MPa, in case of tie arrangement Type-A, lost at least 50% of their load-carrying capacity just after the peak strength. This phenomenon occurs even when $\rho_s \approx 2.1\%$, which is similar with the maximum ρ_s value allowed in RC bridge piers designed in Japan.[4] Specimens with ρ_s of approximately 1.0% started to lose the capacity just after the peak strength, and the machine was unable to continue loading at approximately 1/3 of the peak strength after the peak strength. But, specimens having concrete compressive strength of approximately 120 MPa, in case of tie arrangement Type-B, show the significant increase in ductility even when ρ_s is approximately 1.0%. Therefore, test results indicate that the columns made of HSC is more affected by the tie arrangement than the columns made of NSC for enhancing the strength and ductility.

5. Development of the stress-strain curve

5.1 Formulation of confinement effect

In this study, the effective confining pressure p_e was defined according to Eq. (1).

$$p_e = k_e \rho_w f_{s,cal} \tag{1}$$

where, ρ_w is the area ratio of the lateral tie, $f_{s,cal}$ is the stress in the lateral tie at the concrete peak strength, and k_e is the effective confinement coefficient[10] given by

$$k_e = \left(1 - \sum \frac{(w_i')^2}{6 b_c d_c}\right)\left(1 - \frac{s'}{2b_c}\right)\left(1 - \frac{s'}{2d_c}\right) \Big/ (1 - \rho_{cc}) \tag{2}$$

where, w_i' is the clear spacing between adjacent longitudinal bars in a rectangular section, s' is the clear spacing of ties, b_c and d_c are the width and depth of the concrete core, and ρ_{cc} is the longitudinal bar ratio in the core section.

A regression analysis was performed on all test results to formulate the peak strength f_{cc}, the axial strain at the peak strength ε_{cc}, and the strain at 50% of the peak strength after the peak strength ε_{50}. Eqs. (3)~(5) are obtained from regression analyses of experimental data for the specimens. Origin 6.1 was used for the analyses.

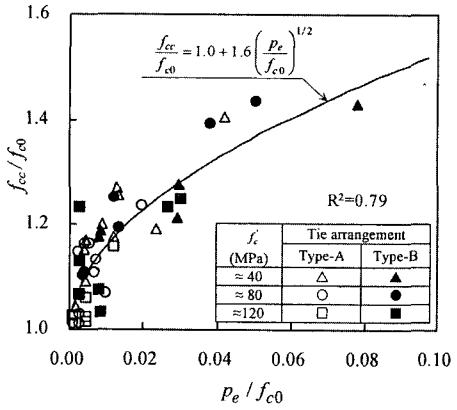

Fig. 8 Relationship between f_{cc}/f_{c0} and p_e/f_{c0}

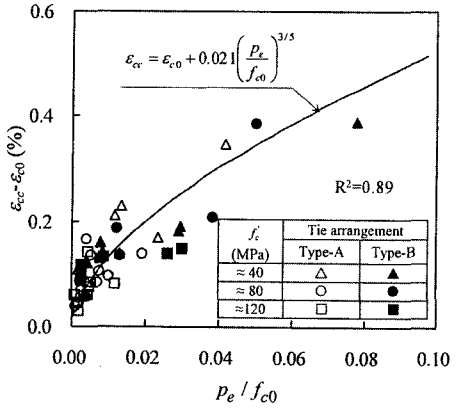

Fig. 9 Relationship between $\varepsilon_{cc} - \varepsilon_{c0}$ and p_e/f_{c0}

$$\frac{f_{cc}}{f_{c0}} = 1.0 + 1.6\left(\frac{p_e}{f_{c0}}\right)^{1/2} \tag{3}$$

$$\varepsilon_{cc} = \varepsilon_{c0} + 0.021\left(\frac{p_e}{f_{c0}}\right)^{3/5} \tag{4}$$

$$\varepsilon_{50} = \varepsilon_{50u} + 30\frac{k_2^2 p_e}{f_{c0}^2} \tag{5}$$

$$f_{c0} = 0.85 f_c' \tag{6}$$

$$\varepsilon_{c0} = 0.0028 - 0.0008 k_1 \tag{7}$$

$$\varepsilon_{50u} = 0.0028 + 0.0007 k_1 \tag{8}$$

$$k_1 = 40/f_{c0} \le 1.0 \tag{9}$$

$$k_2 = 1 + k_e\frac{(f_{sy} - f_{s,cal})}{f_{sy}} \tag{10}$$

where p_e, f_{c0}, and f_{cc} are in MPa, and f_{cc} and ε_{cc} are the peak strength and the corresponding strain of the unconfined concrete, respectively. Also, Eqs. (7) and (9) are suggested by Razvi and Saatcioglu[11] and ε_{c0} and ε_{50u}, respectively, are the strain at the peak strength and the strain at $0.5f_{c0}$ of the unconfined concrete. Figs. 8 and 9

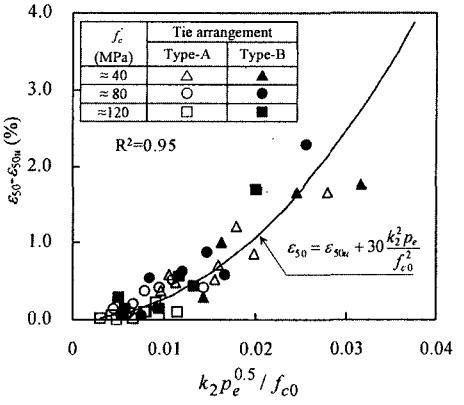

Fig. 10 Relationship between $k_2 p_e^{0.5}/f_{c0}$ and p_e/f_{c0}

are the plots of f_{cc}/f_{c0} versus p_e/f_{c0} and $\varepsilon_{cc} - \varepsilon_{c0}$ versus p_e/f_{c0}, respectively. Meanwhile, Fig. 10 shows the value of $\varepsilon_{50} - \varepsilon_{50u}$ as a function of the value $k_2 p_e^{0.5}/f_{c0}$. In Figs. 8~ 10 including test results from Hong et al.,[2] R^2 represents the correlation coefficient.

5.2 Stress in lateral ties at the concrete peak strength

In this section, the relationship between the lateral confining pressure and lateral strain ε_{cc} is illustrated and a method for calculating the stress $f_{s,cal}$ of the confined concrete is presented. Nielsen,[12] after collecting data from existing triaxial compression experiments on the concrete compressive strength ranging from 40 to 110 MPa, reported that the axial strain at the peak strength and the lateral strain $\varepsilon_{3,p}$ are related by

$$\varepsilon_{cc} = -2.2\varepsilon_{3,p} \tag{11}$$

where, compression has a positive value. This formula is available for a wide range of confining pressures and concrete compressive strengths (i.e., $0 < p/f_c' < 2.0$)

The stress $f_{s,cal}$ can be computed with the following iterative procedure;

i) Using Eq. (1), calculate the effective confining pressure p_e, assuming $f_{s,cal} = f_{sy}$
ii) Estimate the lateral strain $\varepsilon_{3,p}$ with Eqs. (4) and (11)
iii) Assuming that the strain in the lateral tie is equal to $\varepsilon_{3,p}$, evaluate the resulting stress $f_{s,cal}$ using the stress-strain curve of the lateral tie
iv) If $f_{s,cal} < f_{sy}$, recalculate the pressure p_e with the new value of $f_{s,cal}$
v) Repeat steps ii)~iv) until the value of $f_{s,cal}$ converges

Finally, a formula for $f_{s,cal}$ (Eq. (12)) was derived from regression analyses on the parameters (i.e., k_e etc.) used for the previous iterative procedure. Previous test results have shown that lateral confinement improves the strength of confined concrete, which could be calculated as a function of the confining stress by the lateral ties. Namely, the strain in the lateral tie is defined as the summation of unconfined concrete strain at the peak strength and the effect of the confinement parameters, from which we obtain Eq. (12). Using Eq. (12), $f_{s,cal}$ can be calculated to a sufficient degree of accuracy.

$$f_{s,cal} = E_s \left[0.45\varepsilon_{c0} + 6.8\left(\frac{k_e \rho_w}{f_{c0}} \right)^{9/10} \right] \le f_{sy} \quad (12)$$

where, E_s is the modulus of elasticity of lateral ties and is in MPa and $f_{s,cal}$ is equal to f_{sy} or less.

6. Suggested stress-strain curve

6.1 Selection of the basic model equation

Recently, many researchers have modeled the ascending branch of the stress-strain curve of confined concrete. In this paper, the adaptability of previous ascending branch models is also examined. As was anticipated, the difference between the ascending branch models was insignificant. In order to produce a better correlation, the stress-strain model of Fafitis and Shah,[13] which was originally derived as model for the ascending branch of confined HSC, was selected as the basic equation for the ascending branch (the curve OA in Fig. 11). In this study, the descending branch shown as the decreasing exponential curve AB in Fig. 11 was also selected as the basic equation. On the other hand, the difference between descending branch models was apparent. Among these models, the model proposed by Cusson and Paultre[14] is found to represent the best agreement with the descending branch obtained experimentally for confined HSC columns. Hence, the authors decided to use the model of Cusson and Paultre as the basic equation to predict the stress-stain curves of the confined HSC column (the curve AB in Fig. 11). In addition, the initial Young's modulus of the concrete was calculated using a formula proposed by Garrasquillo et al.[15] (i.e., Eq. (15)). Based on the formulation of confinement effect, Eqs. (13) and (16) are used as the stress-strain model equation.

$$f_c = f_{cc}\left[1 - \left(1 - \frac{\varepsilon_c}{\varepsilon_{cc}} \right)^{\alpha} \right] \quad (0 \le \varepsilon_c \le \varepsilon_{cc}) \quad (13)$$

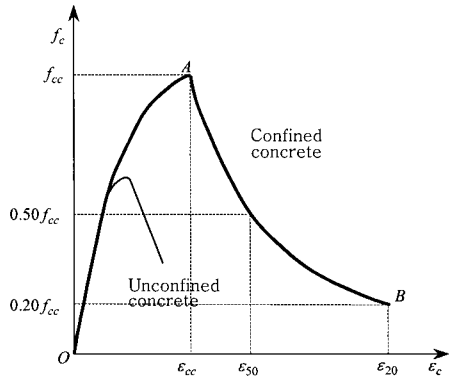

Fig. 11 Stress-strain curves of unconfined concrete and selected basic equation

$$\alpha = E_c \frac{\varepsilon_{cc}}{f_{cc}} \quad (14)$$

$$E_c = 3320\sqrt{f_{c0}} + 6900 \quad (15)$$

$$f_c = f_{cc} \exp\left\{ k_3 (\varepsilon_c - \varepsilon_{cc})^{k_4} \right\} (\varepsilon_{cc} \le \varepsilon_c) \quad (16)$$

$$k_3 = \frac{\ln 0.5}{(\varepsilon_{50} - \varepsilon_{cc})^{k_4}} \quad (17)$$

$$k_4 = 0.3 + 12\frac{k_2 p_e}{f_{c0}} \quad (18)$$

where, f_c and ε_c are the stress and the strain, respectively, in concrete and are in MPa. In addition, k_3 and k_4 are given by Cusson and Paultre.[14] In this paper, k_4 is modified in order to produce a better correlation with test results.

6.2 Verification of the proposed model equation

A comparison of the model to experiment results from 21 specimens is shown in Figs. 12~14. Curves obtained from the models of Li et al.,[5] Cusson and Paultre,[14] and Hoshikuma et al.[16] are also shown in these figures. All curves shown in Figs. 12~14 were developed using the axial strain of square columns with a height-to-width ratio of approximately 3.0. In all cases, the stress-strain relationship proposed from this study accurately predicts the experiment results. Namely, Figs. 12~14 obtained by using $f_{s,cal}$ instead of f_{sy} before the peak strength and f_{sy} and $f_{s,cal}$ after the peak strength in the calculation of confinement effect successfully reproduced the test results.

Existing models show good agreement with this study's columns similar to those tested in their respective experiments. For example, the model of Hoshikuma et al.[16]

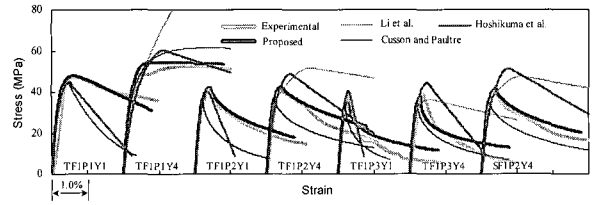

Fig. 12 Comparison of stress-strain curves(f_c' =39.2 MPa)

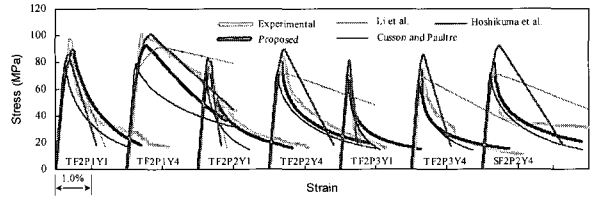

Fig. 13 Comparison of stress-strain curves(f_c' =80.0 MPa)

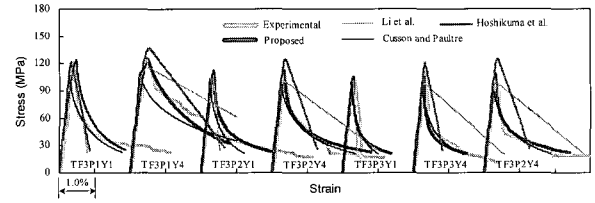

Fig. 14 Comparison of stress-strain curves(f_c' =116.0 MPa)

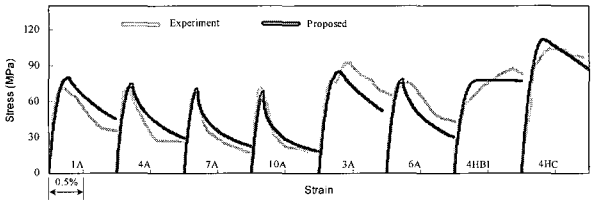

Fig. 15 Comparison of the proposed model equation with existing experimental results

proposed for NSC and lower tie yield strength accurately predicts the behavior of specimens TF1P2Y1 and TF1P3Y1.When normal-strength ties are used, the results of the specimens of group TF2 can also be predicted with sufficient accuracy using the model. Since the models of Li et al.[5] and Hoshikuma et al.[16] use the tie yield strength as the stress in the lateral tie, however, they overestimate the peak strength and the corresponding strain of specimens when f_{sy} is 1420 MPa. On the other hand, since most of Cusson and Paultre's specimens were made with a concrete compressive strength higher than 90 MPa, the models generally underestimate the results of specimens from groups F1 and F2.

6.3 Comparison of the proposed model equation and existing experimental results

Table 3 Li et al.'s experimental results selected for comparison with the proposed equation

Notation	f_c' (MPa)	size (mm)	Lateral tie		
			s (mm)	ρ_s (%)	f_{sy} (MPa)
1A	60.0	240×240 ×720	20	2.63	445
4A	60.0		35	1.50	445
7A	60.0		50	1.05	445
10A	60.0		65	0.80	445
3A	63.0	ϕ240×720	20	1.53	445
6A	63.0		35.5	0.82	445
4HB1	52.0		35	1.67	1318
4HC	82.5		35	1.67	1318

Most experimental research results on stress-strain curves of concrete performed to date are for a ρ_s value greater than 2.0%. Experimental results for low-volumetric ratio lateral ties are thus rare. Fig. 15 shows comparisons between the proposed model equation and Li et al.'s data (Table 3).[5] From this figure, it can be seen that the proposed model represents the experimental results well. Accordingly, it can be concluded that the proposed model equation based on the experimental results of this study is corresponds well with the experimental data obtained from Reference 5. Namely, the proposed equation is reasonably general and accurate.

However, there is a conflict between the proposed model and the experimental data for the peak strengths of specimens 1A and 3A (Fig. 15). Those are attributed to the differences in the volumetric ratio (i.e., 2.63%) and tie arrangement (i.e., circular type) of these two specimens from the specimens in the present study.

7. Conclusions

The following conclusions can be drawn from the experimental and analytical research carried out in this study.

1) High-strength or ultra-high-strength reinforcement has recently been used for lateral ties of reinforced concrete (RC) columns. For square RC columns confined by these lateral ties of low-volumetric ratio, the confinement effect was efficiently improved by changing tie arrangement type from Type-A to Type-B.
2) Based on results from 25 confined columns tested in this study, a method to compute the stress in lateral ties at the concrete peak strength and a stress-strain model were proposed. This model accurately predicts results for both NSC and HSC columns.
3) The results from this study could be widely used for poorly confined high-strength columns, more specifically, for columns with a tie volumetric ratio smaller than 2.0%.

References

1. Han B. S., Shin S. W., and Bahn B. Y., "A model of confined concrete in high-strength reinforced concrete tied columns," *Magazine of Concrete Research*, Vol.55, No.3, 2003, pp. 203~214.
2. Hong K. N., Han S. H., and Yi S. T., "Stress-strain curves of high-strength concrete columns confined by low-volumetric ratio lateral ties," *Engineering Structures*, 2005, (submitted).
3. Structure Committee of New RC Project, "Report of "Development Advanced Reinforced Concrete Buildings Using High-strength Concrete and Reinforcement (New RC Project)", Japan Institute of Construction Engineering, 1993, pp.4~152.
4. Special Committee on Earthquake Disaster Measures, "Specification for Highway Bridges Part V: Seismic Design," Japan Road Association 1997.
5. Li B., Park R. and Tanaka H., "Stress-strain behavior of high-strength concrete confined by ultra-high- and normal-strength transverse reinforcements," *ACI Structural Journal*, Vol.98, No.3, 2001, pp.395~406.
6. Razvi S. and Saatcioglu M., "Circular high-strength concrete columns under concentric compression," *ACI Structural Journal*, Vol.96, No.5, 1999, pp.817~825.
7. Saatcioglu M. and Razvi S., "High-strength concrete columns with square sections under concentric compression," *Journal of Structural Engineering, ASCE*, Vol.124, No.12, 1998, pp.1438~1447.
8. Nakamura H. and Higai T., *Compressive fracture energy and fracture zone length of concrete*, JCI-C51E, 1999, pp. 259~272.
9. Tomosawa F., Noguchi T., and Onoyama K, "Effect of longitudinal of testing machine on compressive strength of concrete," *Proceedings of the Japan Concrete Institute*, Vol.12, No.1, 1990, pp.251~256.
10. Mander J. B., Priestley M. J. N. and Park R., "Theoretical stress-strain model for confined concrete," *Journal of Structural Engineering, ASCE*, Vol.114, No.8, 1988, pp.1804~1826.
11. Razvi S. and Saatcioglu M., "Confinement model for high-strength concrete," *Journal of Structural Engineering, ASCE*, Vol.125, No.3, 1999, pp.281~289.
12. Nielsen C. V., "Triaxial behavior of high-strength concrete and mortar," *ACI Materials Journal*, Vol.95, No.2, 1998, pp. 144~151.
13. Fafitis A. and Shah S. P., *Lateral reinforcement for high-strength concrete columns*, In *High-Strength Concrete*, ACI Special Publication, SP-87. American Concrete Institute, Farmington Hills, MI, USA, 1985, pp.213~232.
14. Cusson D. and Paultre P., " Stress-strain model for confined high-strength concrete," *Journal of Structural Engineering, ASCE*, Vol. 121, No. 3, 1995, pp. 468~477.
15. Garrasquillo R. L., Nilson A. H. and Slate F. O., " Properties of high-strength concrete subjected to short term loads," *ACI Journal*, Vol.78, No.3, 1981, pp.171~178.
16. Hoshikuma J., Kawashima K., and Nagaya K., "A stress-strain model for reinforced concrete columns confined by lateral reinforcement," *Journal of Materials, Concrete Structures and Pavements, JSCE*, Vol.28, No.520, 1995, pp.1~11.